Transparent conducting oxides for advanced photovoltaic applications

John D. Perkins & **David S. Ginley**, National Renewable Energy Laboratory, Golden, Colorado, USA

ABSTRACT

Transparent conducting oxides (TCOs) are a special class of materials that can simultaneously be both optically transparent and electrically conducting and, as such, are a critical component in most thin-film photovoltaics. TCOs are generally based on a limited class of metal oxide semiconductors such In_2O_3, ZnO and SnO_2, which are transparent due to their large band gap energy and can also tolerate very high electronic doping concentrations to yield conductivities of 1000S/cm or higher. However, these three basic TCOs alone do not meet the TCO performance needs of emerging PV and other applications.

Introduction

Transparent conductors in the form of transparent conducting oxides (TCOs) are critical components in many opto-electronic applications including flat panel displays (FPD) and photovoltaics as well as organic electronics including both organic light-emitting diodes (OLED) and organic photovoltaics (OPV) [1,2]. Unlike most metals which are opaque and most transparent materials, which are insulating, TCOs are a special class of wide band gap (~ 3eV) metal oxide semiconductors such as ZnO, SnO_2 and In_2O_3, which can support high enough free electron concentrations (~10^{21}/cm^3) to be effective electrical conductors [3]. Typical good transparent conductors have conductivities of 1000 – 5000S/cm and are transparent from ~ 350 – 1500nm (thereby including the visible portion of the spectrum, 400-700nm). For comparison, we note that copper metal is about 100 times more conductive than a typical TCO. For single-junction PV applications, transparency out to about 850nm is a requirement, which does not put too much of a constraint on TCO materials.

TCOs in photovoltaics

In PV applications, transparent conductors are needed as a contact for collection of the photo-generated carriers while still allowing the light to reach the active solar absorber material. As such, transparent conducting oxides are part of every thin-film photovoltaic technology. The two main PV areas where this is not the case are epitaxial multi-junction III-

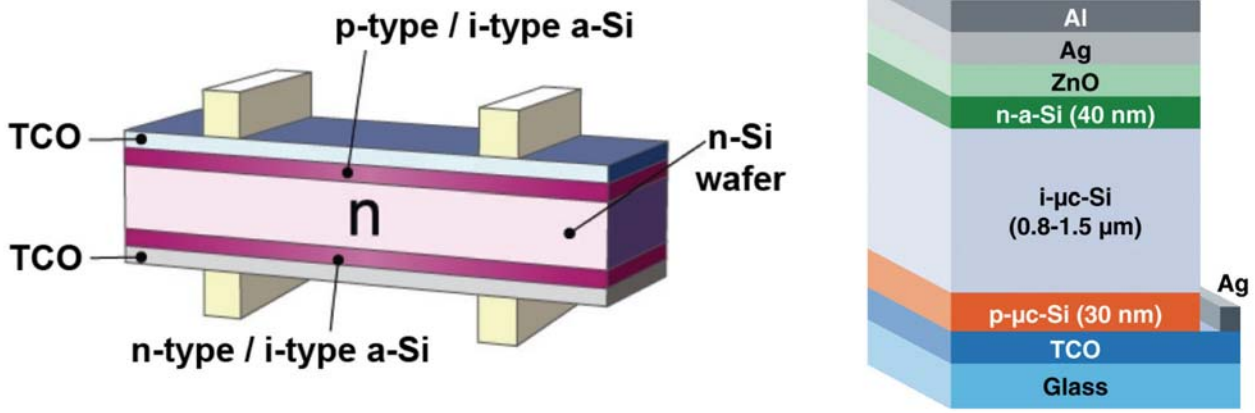

Figure 1. Configurations for Si heterojunction (SHJ) cells with Sanyo HIT cell on the left.

V solar cells (e.g. $GaInP_2/GaAs$) [4] and conventional bulk/polycrystalline Si cells. In these cases, a thin doped top layer of either III-V semiconductor for the former or Si for the latter can provide satisfactory lateral current transport when used in conjunction with a metallic current collection grid. This latter approach is even being integrated with a TCO as discussed later.

Moving onto PV technologies that use TCO contacts, the image on the left of Figure 1 shows the basic structure of a two-sided Sanyo HIT cell (Heterojunction with Intrinsic Thin-layer, [5]). Note the

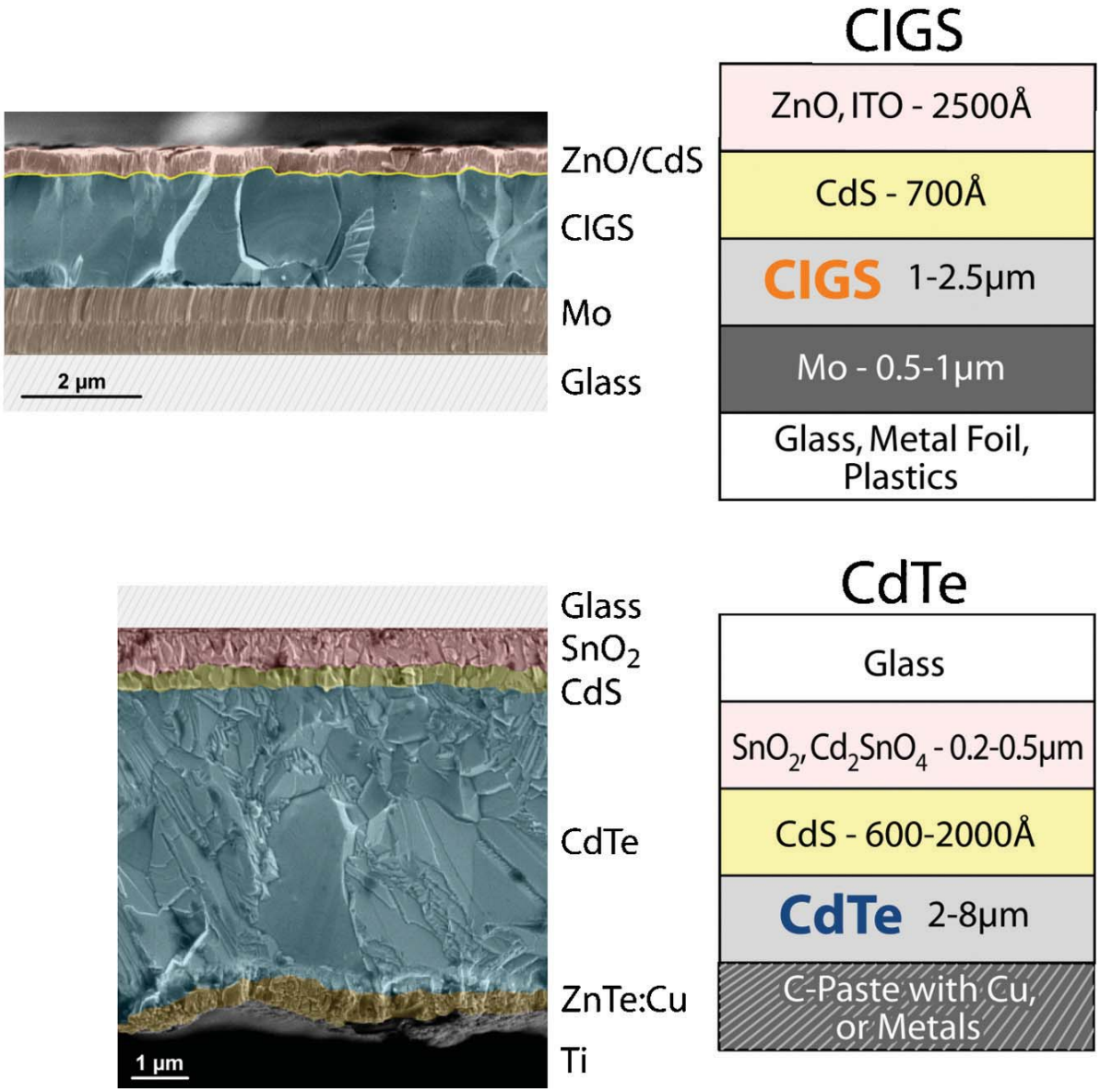

Figure 2. CIGS (top) and CdTe (bottom) PV structures in cross-section.

HORIBA
Scientific

Photovoltaic Improve your Process and Efficiency

HORIBA Scientific offers a full range of analysis equipment for characterization of PV materials including:

- **Efficiency** via **PL**
- **Bulk composition** via **XRF** and **ICP**
- **Surface** and **depth profile analysis** via **GDS**
- **Film thickness** and **n,k** via **Ellipsometry**
- **Stoichiometry variance** via **Raman**

www.photovoltaicstool.com

Featuring:

JOBIN YVON Technology

Find us at www.horiba.com or telephone:

USA:	+1-732-494-8660	France:	+33 (0)1 64 54 13 00
Germany:	+49 (0)62 51 84 750	UK:	+44 (0)20 8204 814
Italy:	+39 02 57603050	Japan:	+81 (0)3 3861 8231
China:	+86 (0)10 8567 9966	Other Countries:	+33 (0)1 64 54 13 00

Look for our new e-mail addresses at HORIBA.com

two TCO layers, one for the top and one for the bottom. The Sanyo-HIT cell is an Si Heterojunction (SHJ) structure which uses thin hydrogenated amorphous Si (a-Si:H) layers in conjunction with a crystalline Si core [6]. The image on the right in Figure 1 shows a more expanded view of a one-sided SHJ structure. Note that even for this structure, there are still two TCO layers. ZnO is part of the top of the TCO/metal multilayer top contact and TCO-coated glass forms the transparent bottom contact for this device. In these SHJ structures, the a-Si layers effectively passivate the c-Si surface, but, due to the low carrier mobility in a-Si, a TCO layer is needed for lateral current conduction to avoid resistive losses. Indium-tin-oxide is typically used in this application [6].

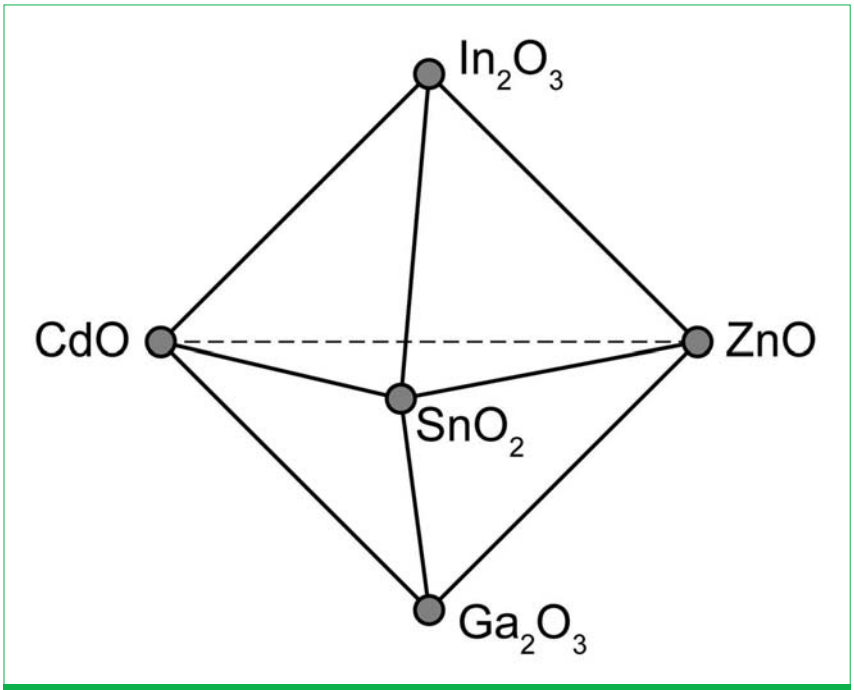

Figure 3. Composition space for conventional TCO materials.

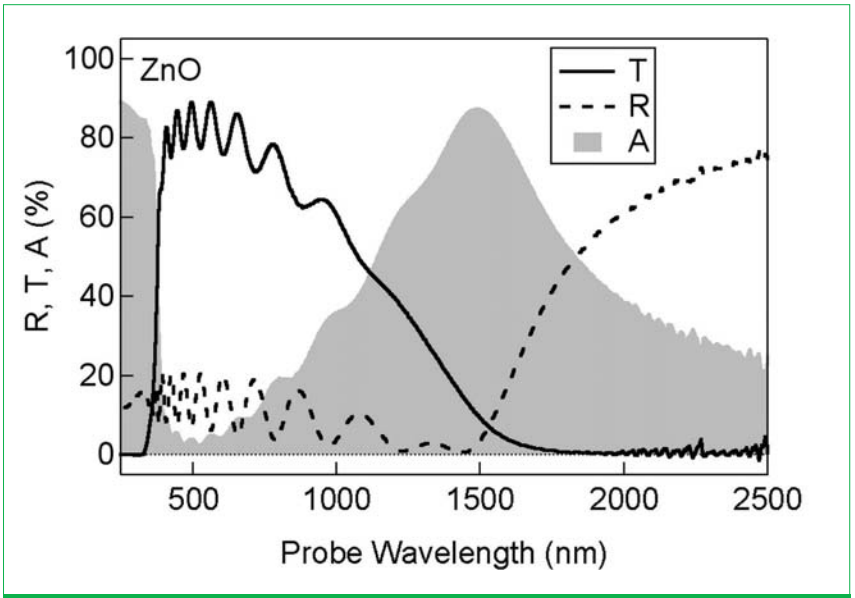

Figure 4. Optical spectra of typical (ZnO) transparent conductor.

> "The range of possible compositions for TCOs is enormous, covering 75% of the tie line between $CdIn_2O_4$ (x = 0) and Cd_2SnO_4 (x=1)."

The upper half of Figure 2 shows a cross-sectional image and schematic for a Cu-In-Ga-Se (CIGS) thin-film solar cell. The primary absorber layer is the CIGS, which has the $CuInSe_2$ structure, but with Ga partially substituted for In to optimize the absorber band gap energy. CdS is deposited over the CIGS to form the junction and then a TCO top layer is used as the transparent electrical contact. In the highest efficiency CIGS cells, a TCO bilayer composed of first undoped ZnO deposited directly onto the CdS layer and then a high conductivity Al-doped ZnO (AZO) on top provides the lateral current conduction [7]. The TCO layer must be deposited at ~ 200°C or lower to avoid degrading the CIGS/CdS junction. Similarly, the lower half of Figure 2 shows a cross-sectional image and schematic for a CdTe/CdS solar cell. In contrast to the CIGS device where the TCO layer is the last layer deposited, the CdTe layer stack begins with TCO coated glass that then becomes the substrate for the subsequent CdS, CdTe and metallic back-contact layers. This allows higher growth temperatures to be used during the TCO layer growth and the F-doped SnO_2 or bilayer Cd_2SnO_4/Zn_2SnO_4 are the standard TCOs for CdTe cells [8,9].

TCO materials and thin-film growth

Figure 3 depicts the conventional five basis set of metal oxides (SnO_2, In_2O_3, ZnO, CdO and Ga_2O_3) which form the majority of crystalline TCOs when appropriately doped. Sn-doped In_2O_3 (ITO), Al-doped ZnO (AZO) and F-doped SnO_2 (FTO) are by far the most commonly used TCO materials at present. CdO can have extraordinarily good electrical properties if neither the yellow colour due to lower band gap energy nor the toxicity of Cd preclude its use. On its own, Ga_2O_3 is not conducting enough to be a practical TCO but it is included as a basis oxide for its role in more complex TCOs such as $GaInO_3$ [10]. Similar binary metal TCO compounds with simple stoichiometries, such as those that lie in the composition space depicted in Figure 3, include Cd_2SnO_4, Zn_2SnO_4, and $In_2Zn_2O_5$ [10,11]. When TCOs formed from three basis oxides are considered, broad ranges of compositions and structures become possible. For examples, in the Cd-In-Sn-O system, $Cd_{1+x}In_{2-2x}Sn_xO_4$ over the range $0 < x < 0.75$ can be made [12]. The range of possible compositions for TCOs is enormous, covering 75% of the tie line between $CdIn_2O_4$ (x = 0) and Cd_2SnO_4 (x=1).

With the exception of CdO, which is light yellow in colour, all of these materials just discussed are inherently transparent in the visible when made undoped and fully oxidized. To achieve practical electrical conductivities of 1000S/cm or greater, these TCO host matrix materials must be effectively doped to create free carrier concentrations on the order of $10^{20} - 10^{21}/cm^3$. The simple single basis oxide materials are almost always made with explicit substitutional doping. Both ZnO and In_2O_3 are usually doped on the

cation site with Al to give $Zn_{1-x}Al_xO$ and Sn to give $In_{2-x}Sn_xO_3$ respectively [13]. SnO_2, on the other hand, is generally doped on the anion site using fluorine to give $SnO_{2-x}F_x$ but it can also be doped on the cation site using Sb [14].

For Al-doped ZnO and Sn-doped In_2O_3, sputtering is the most common method of thin-film deposition. High quality thin films can be grown either by sputtering from ceramic metal oxide targets or by reactive sputtering from metal alloy targets. Other physical vapour deposition (PVD) methods used to deposit these and other TCO materials include evaporation and pulsed laser deposition, a technique which is excellent for proto-typing new materials even if it is not yet practical for large-area commercial deposition. In contrast, SnO_2 is generally deposited using spray pyrolysis or various forms of chemical vapour deposition (CVD). Spray pyrolysis deposited SnO_2:F has been a mainstay of the TCO industry for decades, especially for low-e windows and IR selective windows. We note that PVD-deposited SnO_2 is generally less conducting for reasons that are not fully understood at present [14,15].

Basic opto-electronic properties

Figure 4 shows the optical reflection, transmission and absorption spectra for a typical commercial ZnO TCO on glass. Collectively, these show the key spectral features of a TCO material. First, the material is quite transparent, ~ 80%, in the visible portion of the spectrum, 400 – 700nm. Across this spectral region where the sample is transparent, oscillations due to thin-film interference effects can be seen in both the transmission and reflection spectra. The short wavelength cut off in the transmission at ~ 300nm is due to the fundamental band gap excitation from the valence band to the conduction band of the basis semiconductor, ZnO in this case. The gradual long wavelength decrease in the transmission starting at ~ 1000nm and the corresponding increase in the reflection starting at ~ 1500nm are due to oscillations of the conduction band electrons known as plasma oscillations, or plasmons for short. The corresponding schematic electronic structure for a heavily doped semiconductor with a completely filled lower valence band and significant free electron density in the upper conduction band states is shown in Figure 5. What distinguishes TCOs from conventional semiconductors is that the valence band to conduction band (band gap) energy is very large, 3eV or more, which makes TCO materials transparent in the visible spectrum. Furthermore, TCO materials allow for conduction band free carrier densities as high as 10^{21} electrons/cm^3, which enables the high conductivities.

> "One fundamental reality of TCO materials is that there is an inherent tradeoff between conductivity and the long wavelength transparency limit."

Returning to the optical spectra in Figure 5, there can also be substantial absorption due to these plasma oscillations as is the case for this particular sample with the maximum absorption occurring at the characteristic plasma wavelength, λ_p. As the number of electrons in the conduction band, N, is increased, such as by substitutional doping, the plasma wavelength shifts to shorter wavelengths as $\lambda_p \propto 1/\sqrt{N}$ which also effects the electrical conductivity (σ) since $\sigma = Ne\mu$ where e is the electron charge and μ the electron mobility [16]. Hence, one fundamental reality of TCO materials is that there is an inherent tradeoff between conductivity and the long wavelength transparency limit. At very high electron

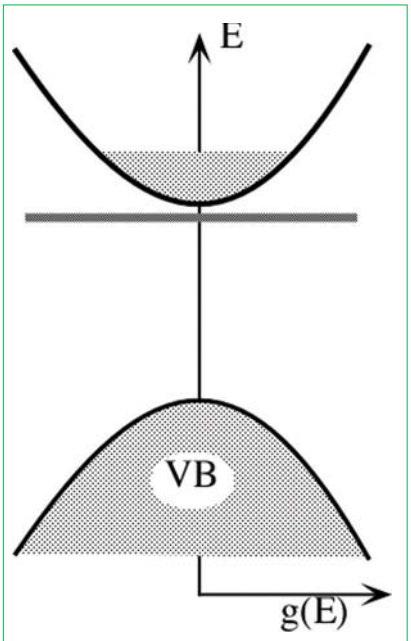

Figure 5. Schematic electronic structure of TCO materials.

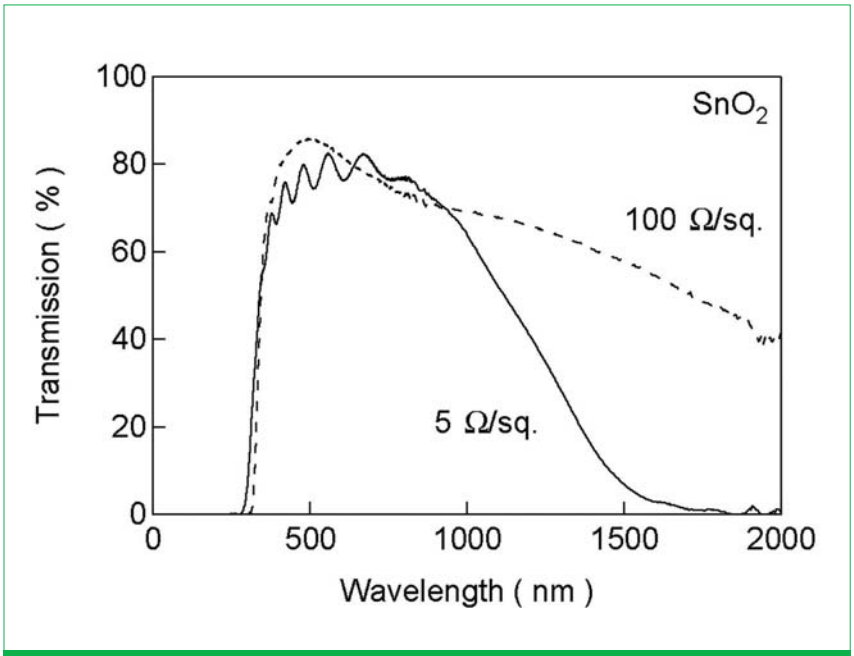

Figure 6. Optical transmission spectra of SnO_2 TCOs with different sheet resistances.

concentrations, this can even decrease the visible wavelength transparency.

For example, Figure 6 shows how the infrared transparency increases for SnO_2 TCOs as the sheet resistance is increased from 5Ω/sq. to 100Ω/sq. Even though both of these SnO_2 samples have similar visible wavelength transparency, the 5Ω/sq. sample would be unusable as a transparent conductor for telecom applications at 1500nm. TCO optimization includes not just the inherent trade-off between conductivity and transparency just discussed, but also many other application-specific constraints such as chemical compatibility, required deposition temperature, stability at the operating temperature and surface roughness, among others. Collectively, these examples should make it clear that there is no such thing as a single 'best' TCO and that TCOs must be tailored to the constraints of the specific application. This includes not just the broad distinction between TCOs for flat panel displays, PV and telecom, but also the distinct TCO requirements for the different thin-film PV technologies. This 'set' of requirements is what is driving the development of new TCO materials in a number of application areas.

Recent materials developments

Three recent trends in new TCO materials research are: 1) The development of high electron mobility materials; 2) The use of amorphous mixed metal oxide TCOs which can be deposited at low or even ambient temperature, and 3) The discovery of TiO_2-based TCOs. The practical industry standard reference point for this new materials development is crystalline ITO with 10wt.% SnO_2 in In_2O_3 deposited at 250 – 350°C which typically has electron mobilities of ~ 30cm^2/V-sec.

Figure 7 shows the electrical conductivity, carrier concentration and electron mobility for Ti-doped In_2O_3 on glass grown by sputtering [17]. Of particular note are the high mobilities, > 80 cm^2/V-sec, observed for films with Ti concentration of 1-2%. This is attributed primarily to the high doping efficiency of Ti in In_2O_3, which is found to be near unity for Ti concentrations near 2%. For comparison, in most ITO the doping efficiency of Sn is about 1 electron per 4 Sn atoms. Mo-doped In_2O_3 is also a high mobility variant on doped indium oxide with mobilities of 60cm^2/V-sec for sputtered films on glass [18] and as high

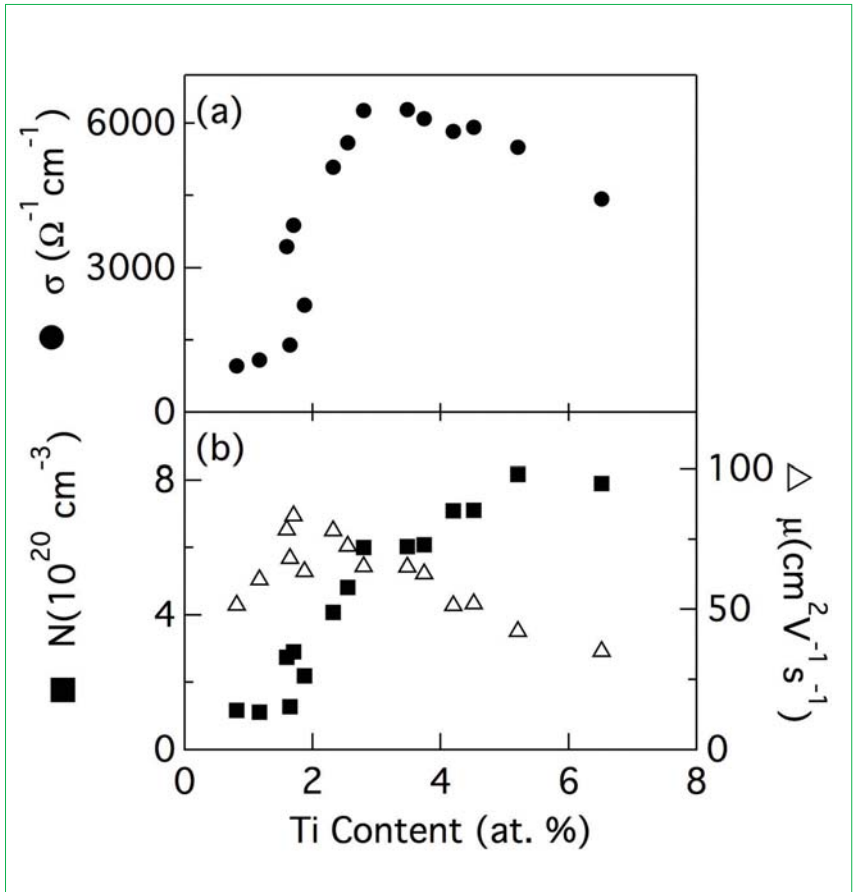

Figure 7. Electrical conductivity (σ), carrier concentration (N) and mobility (μ) of Ti-doped In_2O_3.

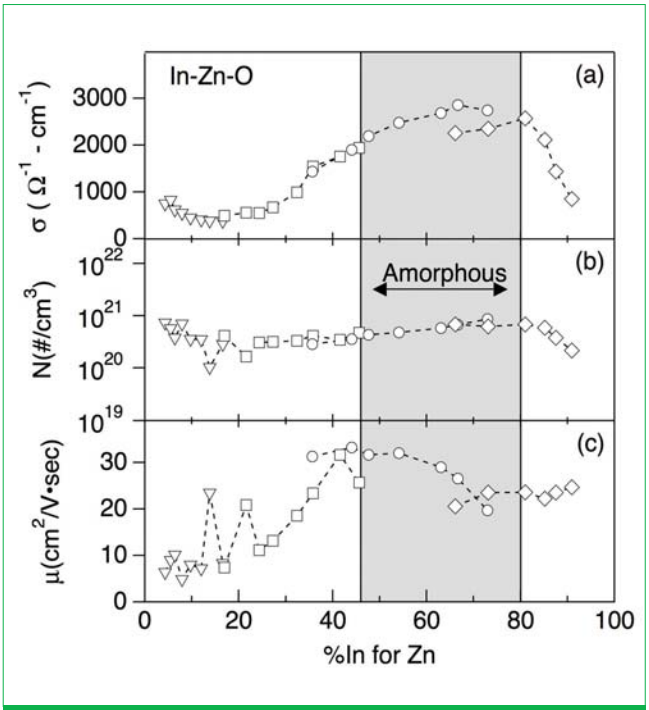

Figure 8. Electrical conductivity (σ), carrier concentration (N) and mobility (μ) of In-Zn-O.

as 125cm^2/V-sec for films deposited by PLD onto single crystal substrates [19]. Interestingly, in this case the doping efficiency is less than half of that for the Ti.

While traditional TCOs are highly crystalline, recently, a new class of amorphous TCO materials, typified by amorphous In-Zn-O (a-IZO) and based on double (or triple) oxides of heavy metal cations with ionic electronic configuration (n-1)d^{10}ns^0 has emerged [20,21]. These materials typically exhibit an electron mobility of 30–60cm^2/V-sec, which is unusually high and is thought to arise from the direct spatial overlap of the large and spherical heavy metal cation ns^0 orbitals and the lack of grain boundaries. For comparison, typical thin-film amorphous Si has mobilities of less than 1cm^2/V-sec. Technologically, a-IZO and similar materials are of great interest because they can be easily deposited onto glass or plastic substrates by ambient temperature sputtering, have excellent optical and electrical properties, are very smooth (R_{RMS} < 0.5nm) and once deposited, do not crystallize until heated to 500°C or higher [22]. Figure 8 shows the electrical conductivity, carrier concentration and electron mobility as a function of metals composition for IZO films grown by composition gradient combinatorial sputtering [23]. Note that broad conductivity maximum with σ ≈ 3000S/cm occurs in the composition range which is amorphous, ~ 55 to 80 at. % indium in this case. While for transparent conductor applications, a high carrier concentration is needed, we note that when grown in the presence of 5 – 10% oxygen, these amorphous mixed metal oxides have carrier concentrations of order 10^{16} – 10^{18}/cm^3 and are being developed as channel layers for transparent thin-film transistors (TTFTs) [24,25]. At present, amorphous In-Ga-Zn-O is the primary material of interest for TTFT applications.

Recently, Nb and Ta-doped TiO_2 have been shown to be good transparent conductors with conductivities of ~ 3000S/cm on single crystal substrates and ~ 2000S/cm on glass [26-28]. The highest conductivity has been observed for the Nb-doped materials and some recent theoretical results support this [29]. In a simple electron counting model for TiO_2, the Ti^{4+} has no electrons in the 3d states, which contradicts the conventional wisdom that metal oxide materials for TCOs should always have filled d-shell states. To obtain these good TCO properties, the TiO_2 must have the anatase structure perhaps due to a much lower effective mass than rutile. The more common rutile TiO_2 is not a good TCO. At present, it is not known whether anatase TiO_2 is the first member of a new general class of TCOs or a singular exception to the filled d-states rule.

Organic PV applications

TCO materials are also critical in organic photovoltaics (OPV), where they can be used in a conventional geometry as shown in Figure 9 or in an inverted geometry where the oxide becomes the electron acceptor. Clearly, these two configurations require very different characteristics for the TCO in terms of electron affinity, surface chemistry and even doping level. A typical layered structure for the conventional bulk heterojunction is shown in Figure 9 where the TCO acts as the hole extraction contact in conjunction with either an organic or inorganic hole transport layer (HTL). In this application, reducing the energy level mismatch between the Fermi level of the TCO and the highest occupied molecular level (HOMO) of the organic semiconductor is believed to be central to improving the current collection and operating voltage. In general, for TCOs used in typical bulk heterojunction OPV (Figure 9), higher work function TCOs are needed to improve the energy level matching [30].

Alternatively, TCOs or similar materials may also have applications as the electron acceptors in an inverted OPV device. In this case, lower work functions TCOs are needed to move the conduction band higher and thus increase the open circuit potential. In these devices, due to the strong exciton binding energy and short exciton diffusion length in organic semiconductors, the photo-excited excitons (electron-hole pairs) can only be effectively split by an interface-induced charge separation, where the electron is transferred from the organic absorber to the acceptor. In this case, TCOs with a higher band gap energy (lower work function) are desired to avoid voltage loss when the electron transfers from the lowest unoccupied molecular orbital (LUMO) of the organic to the TCO conduction band. Figure 10 shows both the band gap energy increase in ZnO (shorter wavelength absorption edge) due to substituting Mg in place of Zn and the corresponding increased open circuit voltage in a simple planer OPV device where Zn(Mg)O is used as the electron acceptor [31]. Overall, the substitution of Mg for Zn in ZnO decreases the band offset between the LUMO of the polymer donor and the conduction band of the acceptor metal oxide material. As shown in the inset, the V_{OC} was increased from 500 to 900mV in the P3HT–$Zn_{1-x}Mg_xO$ devices through the substitution of Mg into ZnO over a range of 0 to 30% Mg for Zn. However, to be effectively incorporated into a practical OPV device, this basic materials result would have to be transferable to an intercalated metal-oxide/organic active layer structure with nanometre-length scales. This remains an active area of research.

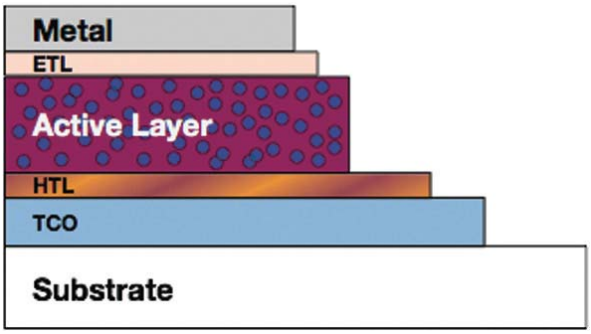

Figure 9. Schematic cross-section of an organic photovoltaic (OPV).

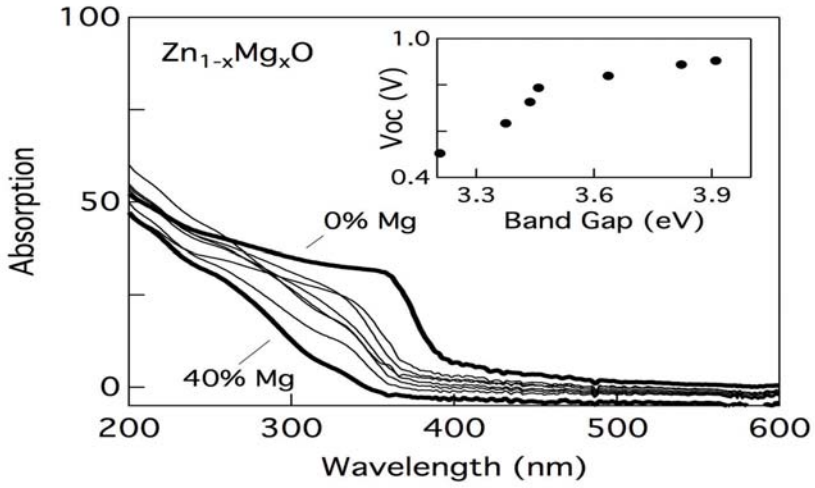

Figure 10. Optical absorption of Mg substituted ZnO. Inset: Effect of TCO band gap on OPV open circuit voltage.

Summary

Thin film photovoltaics require an optically-transparent electrically-conducting contact layer to enable current extraction while allowing sunlight to reach the active PV junction. For most PV applications, this need is met with transparent conducting oxides that are heavily doped wide band gap semiconductors. Crystalline Sn-doped In_2O_3 is the industry standard with Al-doped ZnO and F-doped SnO_2 also being used commercially. However, due to factors such as cost, reactivity, deposition temperature and stability, these three materials are not sufficient to meet the TCO requirements for emerging high performance applications both in PV or other opto-electronic applications. Consequentially, new materials are being actively developed. A few important areas of current TCO materials research include compositionally complex binary, ternary and beyond materials, amorphous mixed metal oxide TCOs, early transition metal series TCOs and higher performance dopants. The past decade has seen a resurgence in TCO research and significant advances are likely in the next five years.

Acknowledgements

This work was supported by the National Center for Photovoltaics (NCPV) at National Renewable Energy Laboratory through the U.S. Department of Energy under Contract No. DE-AC36-99G010337.

References

[1] Ginley, D.S. and Bright, C. 2000, 'Transparent Conducting Oxides', *MRS Bulletin*, 25, p. 15.

[2] Fortunato, E., Ginley, D., Hosono, H. and Paine, D.C. 2007, 'Transparent conducting oxides for photovoltaics', *MRS Bulletin*, 32, p. 242.

[3] Lany, S. and Zunger, A. 2007, 'Dopability, intrinsic conductivity, and nonstoichiometry of transparent conducting oxides', *Physical Review Letters*, 98, Artn 045501.

[4] Bertness, K.A., Kurtz, S.R., Friedman, D.J., Kibbler, A.E., Kramer, C. and Olson, J.M. 1994, '29.5 Percent Efficient GaInP/GaAs Tandem Solar-Cells', *Applied Physics Letters*, 65, p. 989.

[5] Taguchi, M., Kawamoto, K., Tsuge, S., Baba, T., Sakata, H., Morizane, M., Uchihashi, K., Nakamura, N., Kiyama, S. and Oota, O. 2000, 'HIT (TM) cells

- High-efficiency crystalline Si cells with novel structure', *Progress in Photovoltaics*, 8, p. 503.

[6] Branz, H.M., Teplin, C.W., Young, D.L., Page, M.R., Iwaniczko, E., Roybal, L., Bauer, R., Mahan, A.H., Xu, Y., Stradins, P., Wang, T. and Wang, Q. 2008, 'Recent advances in hot-wire CVD R&D at NREL: From 18% silicon heterojunction cells to silicon epitaxy at glass-compatible temperatures', *Thin Solid Films*, 516, p. 743.

[7] Repins, I., Contreras, M.A., Egaas, B., Dehart, C., Scharf, J., Perkins, C.L., To, B. and Noufi, R. 2008, '19.9%-efficient ZnO/CdS/$CuInGaSe_2$ solar cell with 81.2% fill factor', *Progress in Photovoltaics*, 16, p. 235.

[8] Wu, X., Asher, S., Levi, D.H., King, D.E., Yan, Y., Gessert, T.A. and Sheldon, P. 2001, 'Interdiffusion of CdS and Zn_2SnO_4 layers and its application in CdS/CdTe polycrystalline thin-film solar cells', *J. Appl. Phys.*, 89, p. 4564.

[9] Wu, X., Coutts, T.J. and Mulligan, W.P. 1997, 'Properties of transparent conducting oxides formed from CdO and ZnO alloyed with SnO_2 and In_2O_3', *J. Vac. Sci. Technol.*, A, 15, p. 1057.

[10] Minami, T. 2005, 'Transparent conducting oxide semiconductors for transparent electrodes', *Semiconductor Science and Technology*, 20, p. S35.

[11] Freeman, A.J., Poeppelmeier, K.R., Mason, T.O., Chang, R.P.H. and Marks, T.J. 2000, 'Chemical and Thin-Film Strategies for New Transparent Conducting Oxides', *MRS Bulletin*, 25, p. 45.

[12] Kammler, D.R., Mason, T.O., Young, D.L. and Coutts, T.J. 2001, 'Thin films of the spinel $Cd_{1+x}In_{2-2x}Sn_xO_4$ transparent conducting oxide solution', *J. Appl. Phys.*, 90, p. 3263.

[13] Gordon, R.G. 2000, 'Criteria for Choosing Transparent Conductors', *MRS Bulletin*, 25, p. 52.

[14] Stjerna, B., Olsson, E. and Granqvist, C.G. 1994, 'Optical and Electrical Properties of Radio-Frequency Sputtered Tin Oxide Films Doped with Oxygen Vacancies, F, Sb, or Mo', *J. Appl. Phys.*, 76, p. 3797.

[15] Lee, S.U., Choi, W.S. and Hong, B. 2007, 'Synthesis and characterization of SnO_2: Sb film by dc magnetron sputtering method for applications to transparent electrodes', *Physica Scripta*, T129, p. 312.

[16] Perkins, J.D., Teplin, C.W., Van Hest, M.F.A.M., Alleman, J.L., Li, X., Dabney, M.S., Keyes, B.M., Gedvilas, L.M., Ginley, D.S., Lin, Y. and Lu, Y. 2004, 'Optical analysis of thin film combinatorial libraries', *Applied Surface Science*, 223, p. 124.

[17] Van Hest, M.F.A.M., Dabney, M.S., Perkins, J.D., Ginley, D.S. and Taylor, M.P. 2005, 'Titanium-doped indium oxide: A high-mobility transparent conductor', *Applied Physics Letters*, 87, Artn 032111.

[18] Van Hest, M.F.A.M., Dabney, M.S., Perkins, J.D. and Ginley, D.S. 2006, 'High-mobility molybdenum doped indium oxide', *Thin Solid Films*, 496, p. 70.

[19] Warmsingh, C., Yoshida, Y., Readey, D.W., Teplin, C.W., Perkins, J.D., Parilla, P.A., Gedvilas, L.M., Keyes, B.M. and Ginley, D.S. 2004, 'High-mobility transparent conducting Mo-doped In_2O_3 thin films by pulsed laser deposition', *J. Appl. Phys.*, 95, p. 3831.

[20] Hosono, H., Nomura, K., Ogo, Y., Uruga, T. and Kamiya, T. 2008, 'Factors controlling electron transport properties in transparent amorphous oxide semiconductors', *Journal of Non-Crystalline Solids*, 354, p. 2796.

[21] Hosono, H., Yasukawa, M. and Kawazoe, H. 1996, 'Novel oxide amorphous semiconductors: Transparent conducting amorphous oxides', *Journal of Non-Crystalline Solids*, 203, p. 334.

[22] Taylor, M.P., Readey, D.W., Van Hest, M.F.A.M., Teplin, C.W., Alleman, J.L., Dabney, M.S., Gedvilas, L.M., Keyes, B.M., To, B., Perkins, J.D. and Ginley, D.S. 2008, 'The Remarkable Thermal Stability of Amorphous In-Zn-O Transparent Conductors', *Advanced Functional Materials*, 18, p. 3169.

[23] Taylor, M.P., Readey, D.W., Teplin, C.W., Van Hest, M.F.A.M., Alleman, J.L., Dabney, M.S., Gedvilas, L.M., Keyes, B.M., To, B., Perkins, J.D. and Ginley, D.S. 2005, 'The electrical, optical and structural properties of $In_xZn_{1-x}O_y$ ($0 <= x <= 1$) thin films by combinatorial techniques', *Measurement Science and Technology*, 16, p. 90.

[24] Nomura, K., Ohta, H., Takagi, A., Kamiya, T., Hirano, M. and Hosono, H. 2004, 'Room-temperature fabrication of transparent flexible thin-film transistors using amorphous oxide semiconductors', *Nature*, 432, p. 488.

[25] Dehuff, N.L., Kettenring, E.S., Hong, D., Chiang, H.Q., Wager, J.F., Hoffman, R.L., Park, C.H. and Keszler, D.A. 2005, 'Transparent thin-film transistors with zinc indium oxide channel layer', *J. Appl. Phys.*, 97.

[26] Hitosugi, T., Ueda, A., Nakao, S., Yamada, N., Furubayashi, Y., Hirose, Y., Shimada, T. and Hasegawa, T. 2007, 'Fabrication of highly conductive $Ti_{1-x}Nb_xO_2$ polycrystalline films on glass substrates via crystallization of amorphous phase grown by pulsed laser deposition', *Applied Physics Letters*, 90, Artn 212106.

[27] Gillispie, M.A., Van Hest, M.F.A.M., Dabney, M.S., Perkins, J.D. and Ginley, D.S. 2007, 'rf magnetron sputter deposition of transparent conducting Nb-doped TiO_2 films on $SrTiO_3$', *J. Appl. Phys.*, 101, Artn 033125.

[28] Furubayashi, Y., Hitosugi, T., Yamamoto, Y., Inaba, K., Kinoda, G., Hirose, Y., Shimada, T. and Hasegawa, T. 2005, 'A transparent metal: Nb-doped anatase TiO_2', *Applied Physics Letters*, 86.

[29] Osorio-Guillen, J., Lany, S. and Zunger, A. 2008, 'Atomic control of conductivity versus ferromagnetism in wide-gap oxides via selective doping: V, Nb, Ta in anatase TiO2', *Physical Review Letters*, 100, 036601.

[30] Shaheen, S.E., Ginley, D.S. and Jabbour, G.E. 2005, 'Organic-based photovoltaics. toward low m-cost power generation', *Mrs Bulletin*, 30, p. 10.

[31] Olson, D.C., Shaheen, S.E., White, M.S., Mitchell, W.J., Van Hest, M., Collins, R.T. and Ginley, D.S. 2007, 'Band-offset engineering for enhanced open-circuit voltage in polymer-oxide hybrid solar cells', *Advanced Functional Materials*, 17, p. 264.

About the Authors

John Perkins is a Senior Scientist in the National Center for Photovoltaics at the National Renewable Energy Laboratory in Golden, Colorado, USA. He received his Ph.D. in physics in 1994 from MIT. His current research focuses on thin-film transparent conductors and combinatorial approaches to material science research.

David Ginley is a research fellow and group manager in the National Center for Photovoltaics at the National Renewable Energy Laboratory. He received his Ph.D. in inorganic chemistry in 1976 from MIT. Research interests include nanomaterials, transparent conductive oxides, organic photovoltaics, combinatorial materials science and new process technologies for solar energy conversion.

Enquiries

John Perkins
National Renewable Energy Laboratory
1617 Cole Blvd.
Golden
CO 80401
USA

Email: john.perkins@nrel.gov